Scattering of NH3 and ND3 with rare gas atoms at low collision energy

J. Loreau and A. van der Avoird

Citation: The Journal of Chemical Physics **143**, 184303 (2015); doi: 10.1063/1.4935259
View online: http://dx.doi.org/10.1063/1.4935259
View Table of Contents: http://scitation.aip.org/content/aip/journal/jcp/143/18?ver=pdfcov
Published by the AIP Publishing

Scattering of NH_3 and ND_3 with rare gas atoms at low collision energy

J. Loreau[1,a)] and A. van der Avoird[2,b)]
[1]*Service de Chimie Quantique et Photophysique, Université Libre de Bruxelles (ULB) CP 160/09, 50 av. F.D. Roosevelt, 1050 Brussels, Belgium*
[2]*Theoretical Chemistry, Institute for Molecules and Materials, Radboud University, Heyendaalseweg 135, 6525 AJ Nijmegen, The Netherlands*

(Received 2 September 2015; accepted 26 October 2015; published online 11 November 2015)

We present a theoretical study of elastic and rotationally inelastic collisions of NH_3 and ND_3 with rare gas atoms (He, Ne, Ar, Kr, Xe) at low energy. Quantum close-coupling calculations have been performed for energies between 0.001 and 300 cm^{-1}. We focus on collisions in which NH_3 is initially in the upper state of the inversion doublet with $j = 1, k = 1$, which is the most relevant in an experimental context as it can be trapped electrostatically and Stark-decelerated. We discuss the presence of resonances in the elastic and inelastic cross sections, as well as the trends in the inelastic cross sections along the rare gas series and the differences between NH_3 and ND_3 as a colliding partner. We also demonstrate the importance of explicitly taking into account the umbrella (inversion) motion of NH_3 in order to obtain accurate scattering cross sections at low collision energy. Finally, we investigate the possibility of sympathetic cooling of ammonia using cold or ultracold rare gas atoms. We show that some systems exhibit a large ratio of elastic to inelastic cross sections in the cold regime, which is promising for sympathetic cooling experiments. The close-coupling calculations are based on previously reported *ab initio* potential energy surfaces for NH_3–He and NH_3–Ar, as well as on new, four-dimensional, potential energy surfaces for the interaction of ammonia with Ne, Kr, and Xe, which were computed using the coupled-cluster method and large basis sets. We compare the properties of the potential energy surfaces corresponding to the interaction of ammonia with the various rare gas atoms. © *2015 AIP Publishing LLC.* [http://dx.doi.org/10.1063/1.4935259]

I. INTRODUCTION

The theoretical study of ammonia-rare gas (NH_3–Rg) complexes has historically been motivated by the study of rotational energy transfer as well as by the large amount of experimental data on the microwave and infrared spectra. In this context, the most studied systems are NH_3–He and NH_3–Ar. Collisions of NH_3 or ND_3 with helium are of importance in the modeling of various astrophysical environments such as the interstellar medium and have thus been investigated both theoretically[1–3] and experimentally.[4,5] On the other hand, the NH_3–Ar complex has been the subject of numerous studies that focused either on its spectra[6–9] or on the collision dynamics through the measurement and analysis of integral and differential cross sections.[10–15] Although the literature is less extensive regarding the other NH_3–Rg complexes, these systems have also been studied experimentally in spectroscopic[16–19] or molecular beam experiments.[20,21]

Recent advances on the manipulation and control of molecular beams have renewed interest in these systems. Measurements of rotationally inelastic, quantum-state resolved, differential cross sections were realized using a hexapole-focused beam of ND_3 molecules colliding with various rare gases (Rg's) or molecular hydrogen.[20,22–24] In these crossed beam scattering experiments, velocity map imaging (VMI) with resonance enhanced multi-photon ionization (REMPI) detection is used to obtain state-to-state differential cross sections (DCSs) that can be directly compared to theoretical predictions based on accurate potential energy surfaces and quantum-mechanical scattering calculations. This provides a good check of the quality of the potential energy surface (PES) due to the sensitivity of the DCSs to the interaction potential. The same techniques, combined with a Stark-decelerated beam of NH_3 or ND_3, will allow the measurement of integral and differential state-to-state cross sections at low collision energies, where the cross sections are dominated by resonances. The low energy ($E < 100$ cm^{-1}) scattering of NH_3 or ND_3 colliding with He and H_2 has recently been explored theoretically[25,26] with a particular emphasis on the resonance structure of the cross section as a function of the collision energy. Moreover, this type of experiment has an excellent energy resolution,[27] which allows a detailed comparison with the theory and provides a stringent test for *ab initio* methods. In an experiment realized with a Stark-decelerated or hexapole-selected beam, only the low-field seeking states are focused.[28] This provides a beam of molecules in a single quantum state, which for ammonia is the upper level of the inversion doublet of ground state *para*-ammonia, i.e., the 11− state.

Elastic and inelastic collisions of NH_3 with He and Ne are also of interest in the context of buffer gas cooling.[29] In order to understand the thermalization of a beam of molecules such as ammonia in a buffer gas cell, as well as the final distribution of the rotational states, detailed knowledge of the scattering cross sections is required. For example, the rotational cooling

a)Electronic mail: jloreau@ulb.ac.be
b)Electronic mail: A.vanderAvoird@theochem.ru.nl

of ammonia seeded into a helium supersonic jet was recently modeled by taking into account rotationally inelastic NH_3–He collisions.[30]

The recent report of the experimental trapping of cold ground state argon atoms[31] also suggests that the sympathetic cooling of molecules such as ammonia might be realized by thermalizing collisions with rare gases. The possibility of sympathetically cooling NH_3 using laser-cooled alkali atoms has been investigated previously[32] but the potential energy surfaces for these systems were deemed too anisotropic. To examine whether this would be feasible using rare gases requires a detailed knowledge of elastic and inelastic cross sections at low collision energy.

The cornerstone of the theoretical study of collision dynamics is an accurate PES. PESs for the interaction of NH_3 with helium[25] and argon[33] that include a dependence on the inversion coordinate of NH_3 have recently been reported. While a few *ab initio* studies have been performed on the interaction of ammonia with the other rare gases,[16,18,32,34,35] they did not include a description of the long-range potential that is required for low-energy scattering.

In this paper, we report new four-dimensional PESs for the interaction of NH_3 with Ne, Kr, and Xe obtained with similar *ab initio* methods as the recently reported PESs for NH_3–He and NH_3–Ar. In Sec. II, we discuss the methods employed and we discuss the main features of the PESs as well as the trends along the rare gas series. In Sec. III, we employ these PESs to investigate the scattering of NH_3 and ND_3 with rare gas atoms. We focus on the initial state 11− of ammonia, which can be trapped electrostatically and Stark decelerated. We compute elastic and inelastic cross sections at energies in the range 0.001–300 cm^{-1} by means of the quantum-mechanical close-coupling method. We discuss the trends in the cross sections for the various rare gas atoms, and we show the importance of taking the full inversion (umbrella) motion NH_3 into account at low energy. Finally, we investigate the possibility of sympathetic cooling NH_3 using rare gas atoms.

II. POTENTIAL ENERGY SURFACES

A. *Ab initio* calculations

Several *ab initio* and semi-empirical PESs for the interaction of ammonia with rare gas atoms have been presented in the literature. Four-dimensional PESs for the van der Waals complexes NH_3–He and NH_3–Ar have recently been computed in our groups using the coupled-cluster method with AVQZ basis sets (see Refs. 25 and 33 and references therein for a comparison with previous work). Calculations for NH_3–Ne,–Kr, and –Xe have also been performed with various *ab initio* methods.[16,18,32,34–36] However, these calculations have been restricted to the region close to the van der Waals minimum, and no complete PESs, including the long-range part of the potential, are available. This will limit the accuracy in calculations of scattering cross sections at low energies. Moreover, it should be noted that these previous studies did not consider the dependence of the PES on the inversion motion of NH_3 in the complex.

In most calculations on NH_3–atom and NH_3–molecule scattering, ammonia is considered to be rigid, as the collision energies considered are smaller than the energy of the various vibrational modes. It is, however, important to consider the possibility of NH_3 inversion (or umbrella motion, corresponding to the ν_2 mode) which induces a splitting of 0.79 cm^{-1} in the ground vibrational level due to tunnelling. This is usually taken into account by means of a model that expresses the inversion wave functions as linear combinations of the equilibrium structures[1,37] (see Sec. III A). While this approximation has been shown to be accurate in the calculation of scattering cross sections at higher energies,[11,25] one can expect the inversion motion to affect the cross sections when the collision energy becomes comparable to the splitting. For the reasons described above, and in order to make a detailed comparison between the Rg's, we computed the PESs corresponding to the interaction of NH_3 with Ne, Kr, and Xe. We chose to take the inversion coordinate into account explicitly.

The interaction energy was computed as a function of four coordinates $(R', \theta', \varphi', \rho')$. The R' coordinate is the length of the vector $\mathbf{R}'$ that connects the N atom to the Rg atom, θ' is the angle between the vector $\mathbf{R}'$ and the ammonia C_3 axis, φ' is the angle of rotation of this vector around the C_3 axis, while ρ' is the umbrella or inversion angle, defined as the angle between the C_3 axis of ammonia and the N–H bonds (see Fig. 1 in Ref. 33 for an illustration of the coordinate system). For $\theta' = 0$ or π, the complex has orientation Rg–NH_3 or Rg–H_3N, respectively. For $\varphi' = 0$, the Rg is in the plane formed by the C_3 axis and one of the N–H bonds, while for $\varphi' = \pi/3$, it is located at equal distance between two hydrogen atoms. The C_{3v} symmetry of NH_3 is conserved throughout our calculations. The N–H bond r length was fixed at its vibrationally averaged value, $r_0 = 1.9204\ a_0$, as calculated in Ref. 33.

The PESs were computed by means of the coupled-cluster method with single, double, and perturbative triple excitations (CCSD(T))[38] with a Hartree-Fock reference wave function using the MOLPRO 2012.1 program.[39] The performance of various basis sets was examined for NH_3–Ar in Ref. 33, and it was established that the aug-cc-pVQZ (or AVQZ) basis set supplemented by a set of diffuse midbond functions provided an excellent accuracy. The PESs were therefore computed with the AVQZ basis set for all atoms,[40] to which we added a set of $(3s3p2d2f1g)$ midbond functions[41] which has been shown to give accurate results for interactions involving rare gases. For Kr and Xe, the core electrons were described by means of relativistic pseudopotentials.[42] The basis set superposition error was accounted for at all geometries using the counterpoise method.[43] In our calculations, the $2s^2 2p^3$ electrons of the N atom, the $1s$ electrons of the H atoms, and the $ns^2 np^6$ electrons of the Rg atom (16 electrons in total) were correlated in the CCSD(T) calculations. The correlation contribution of the outer-core electrons to the interaction energy was found to be less than 0.4% in the case of NH_3–Ar[33] and it is thus neglected in the present study, even though the effect is expected to increase for the heavier rare gases Kr and Xe.[44] The value of the T1 diagnostic[45–47] was inferior to 0.01 for all geometries and all rare gas species,

which demonstrates the single-reference character of the wave function.

The grid used for the *ab initio* calculations was constructed as follows. For θ', the grid consisted of 11 Gauss-Legendre points from 0 to π, while for φ', we used a Gauss-Chebyshev grid of 4 points from 0 to $\pi/3$. This is the same angular grid that was previously employed for NH_3–He and NH_3–Ar. For $\rho' \geq \pi/2$, we used an equidistant grid of 7 points for Ne and 5 points for Kr and Xe. All other geometries can be obtained by symmetry. Finally, for the intermolecular distance R', we used a grid of 34 points for Ne ($3.5 \leq R' \leq 35\ a_0$), 31 points for Kr ($4 \leq R' \leq 30\ a_0$), and 28 points for Xe ($4 \leq R' \leq 28.5\ a_0$). We used a constant spacing of 0.2–0.3 a_0 in the short-range, while in the long-range, the spacing increased progressively. The larger number of grid points for NH_3–Ne results from the fact that we found it necessary to include additional points in the long-range in order to obtain a satisfactory fit of the PES (see below). In total, we computed 10 472 points for the NH_3–Ne PES, 6820 points for the NH_3–Kr PES, and 6160 points for the NH_3–Xe PES. The complete set of *ab initio* energies is available as supplementary material.[48]

In bound state or scattering calculations, the matrix elements of the intermolecular potential between angular momentum basis functions are required. Their evaluation is facilitated if the potential is expanded in tesseral harmonics S_{lm}, i.e., real combinations of spherical harmonics,

$$V(R',\theta',\varphi',\rho') = \sum_{l,m} v_{lm}(R',\rho') S_{lm}(\theta',\varphi'). \tag{1}$$

We only used the tesseral harmonics with $m \geq 0$, i.e., functions of cosine type, which are defined as $S_{lm} = \frac{1}{\sqrt{2}}\left(Y_l^{-m} + (-1)^m Y_l^m\right)$ for $m > 0$ and $S_{l0} = Y_l^0$ in terms of the spherical harmonics Y_l^m. The sum over l runs from 0 to 10, while the sum over $0 \leq m \leq l$ contains only terms for which m is a multiple of 3 due to the threefold symmetry axis of NH_3. We employed the same method as in Ref. 33 to fit the expansion coefficients $v_{lm}(R',\rho')$. In the interaction region, we used two-dimensional cubic splines. In the asymptotic region, we fitted the expansion coefficients at the last three points of the grid in R' to an analytical expression consisting of an inverse power expansion in R' and a polynomial expansion in ρ',

$$v_{lm}(R',\rho') = \sum_{n,p} c_{lmnp} \left(\rho' - \frac{\pi}{2}\right)^p R'^{-n}. \tag{2}$$

We retained the first two terms in the expansion in inverse powers of R' ($n = n_i$ and $n = n_i + 2$, where n_i depends[25] on the value of l) and ten terms in the polynomial expansion in ρ' with $0 \leq p \leq 9$. Since the functions $v_{lm}(R',\rho')$ are even or odd functions of $\left(\rho' - \frac{\pi}{2}\right)$ according to the parity of $l + m$, only terms with p even or odd appear in Eq. (2) and the sum reduces to five terms. Each function v_{lm} is therefore represented by 10 coefficients c_{lmnp}. We obtained a good representation of the asymptotic PES by including only terms up to $l = 5$.

Finally, we note that scattering calculations require that the PES be evaluated in a coordinate system (R,θ,φ,ρ) with the origin at the center of mass of NH_3 rather than on N. The transformation from one coordinate system to the other is straightforward (see Ref. 33) but requires a re-expansion of the PES in terms of these new coordinates. Similarly, in order to treat collisions of ND_3 with rare gases, the coordinate system must also be modified to reflect the shift in the position of the center of mass of the molecule. We assume here that apart from this shift, the PES is the same for the interaction of NH_3 or ND_3 with rare gases, which amounts to neglecting the minor change in r_0 between the two isotopes. In what follows, we only use the center of mass coordinates.

B. Analysis of the PES

The main characteristics of the NH_3–Rg PESs have previously been identified[33,36,49] and it has also been shown that the PESs for all these complexes share the same qualitative features.[36] In particular, it is well known that the minimum of the PES occurs for $\varphi = 60°$, i.e., when the rare gas atom is located between two hydrogen atoms.

The equilibrium geometries and dissociation energies are given in Table I. Several points can be observed. The first is that the dissociation energy D_e increases with the size of the rare gas atom, as expected since the larger Rg's are more polarizable. The second is the increase in the equilibrium distance R_e with the Rg size, which is also expected as the atomic radius is larger for the heavier Rg. Finally, we note that θ_e decreases with increasing Rg size, which is due to the fact that the larger Rg's have a larger electronic cloud that induces a repulsion by the hydrogen atoms. The values presented in Table I agree well with the values reported by Bistoni *et al.* based on a CCSD(T) geometry optimization.[36]

There are three saddle points that hinder internal rotation of NH_3 in the complexes. The first (S_1) occurs for $\varphi = 0$ and hinders rotation along the φ coordinate. The other two (S_2 and S_3) correspond to $\theta = 0°$ and $\theta = 180°$, respectively. We recall that $\theta = 0°$ corresponds to the Rg–NH_3 configuration, while $\theta = 180°$ corresponds to the NH_3–Rg configuration. For both geometries, the NH_3–Rg complex has C_{3v} symmetry. The geometries of these saddle points are given in Table II along with the corresponding energy above the global minimum of the complex (potential barriers). At the S_1 geometry, the Rg atom is in the plane formed by the C_3 axis and a N–H bond, it thus cannot approach NH_3 as closely as for $\varphi = 60°$, and the equilibrium distance is increased. For the same reason, the equilibrium angle θ is much smaller in this geometry than for the global minimum. The barrier preventing rotation about the C_3 axis is seen to reach a plateau for Ar, Kr, and Xe.

By comparing S_2 and S_3, we observe that the configuration with $\theta = 0°$ is always more favorable than $\theta = 180°$, implying

TABLE I. Global minimum of the PES.

Rg	R_e (a_0)	θ_e (deg)	D_e (cm^{-1})
He	6.10	89.0	35.08
Ne	6.23	87.5	66.81
Ar	6.76	85.1	147.6
Kr	6.99	83.0	173.6
Xe	7.35	79.9	197.7

TABLE II. Geometries (R in a_0, θ in degrees) and energy above the global minimum (in cm^{-1}) of the three saddle points of the NH_3–Rg PESs.

	$S_1(\varphi = 0)$			$S_2(\theta = 0°)$		$S_3(\theta = 180°)$	
Rg	R	θ	E	R	E	R	E
He	6.74	82.4	10.34	7.30	21.56	7.34	23.34
Ne	6.75	77.2	16.03	7.02	29.61	7.03	34.15
Ar	7.19	74.1	29.51	7.30	43.91	7.35	57.30
Kr	7.36	65.8	32.25	7.46	39.76	7.55	60.17
Xe	7.64	46.3	31.88	7.74	32.32	7.89	62.44

TABLE III. Parameters of the isotropic component $v_{00}(R, \rho_e)/\sqrt{4\pi}$ of the NH_3–Rg PES, and comparison with the experimental values from Ref. 21.

	R_m (a_0)		ε_m (cm^{-1})		C_6 ($E_h a_0^6$)	
Rg	Theoretical	Expt.	Theoretical	Expt.	Theoretical	Expt.
He	6.83	6.99	19.17	19.76	11.61	10.5
Ne	6.79	6.94	44.56	44.76	24.97	22.8
Ar	7.20	7.24	111.5	109.7	79.86	71.8
Kr	7.43	7.45	136.1	142.8	113.6	111
Xe	7.77	7.77	159.3	173.4	167.4	174

that the Rg atom prefers to be close to the lone pair of N rather than to the hydrogen atoms. While the potential barrier at $\theta = 180°$ increases with the size of the Rg atom, the barrier at $\theta = 0°$ is of maximum height for argon and decreases for the larger Rg atoms.

In Fig. 1, we show the four dominant terms $v_{lm}(R)$ in the expansion of potential (1) for the equilibrium value of ρ, $\rho_e = 112.1°$, and for all Rg atoms. These expansion functions will be used in Sec. III to interpret the relative magnitudes of scattering cross sections. The isotropic term $v_{00}(R)/\sqrt{4\pi}$ has a well that is substantially less deep than the well in the full potential. The equilibrium distances R_m and depths ϵ_m of the isotropic component of the potential are given in Table III together with the corresponding C_6 coefficients. These values can be compared to those obtained by Pirani *et al.* from high resolution molecular beam experiments in which the elastic cross sections for NH_3–Rg scattering were measured.[21] There is good agreement with the present values for all parameters, except for NH_3–Xe where the discrepancy in the value of ϵ_m is somewhat larger.

III. SCATTERING CALCULATIONS

A. Theory

The general theory of quantum inelastic scattering between a rigid symmetric top and an atom has been described in detail in the literature.[1] When the inversion coordinate ρ is taken into account explicitly, the Hamiltonian of the complex can be written as[50]

$$\hat{H} = \sum_i \frac{\hat{j}_i^2}{2I_{ii}(\rho)} + \hat{T}(\rho) + V_{\text{umb}}(\rho) - \frac{\hbar^2}{2\mu R}\frac{\partial^2}{\partial R^2}R + \frac{1}{2\mu R^2}(\hat{J}^2 + \hat{j}^2 - 2\hat{\mathbf{j}}\cdot\hat{\mathbf{J}}) + V(\rho, R, \theta, \varphi), \quad (3)$$

where μ is the reduced mass of the system, $\hat{\mathbf{j}}$ is the angular momentum operator of NH_3, and $\hat{\mathbf{J}}$ is the total angular momentum operator. The first three terms of the Hamiltonian describe the motion of the NH_3 monomer. The sum in the first term runs over $i = x, y, z$ and $I_{ii}(\rho)$ are the principal moments of inertia of NH_3. The second term is the kinetic operator

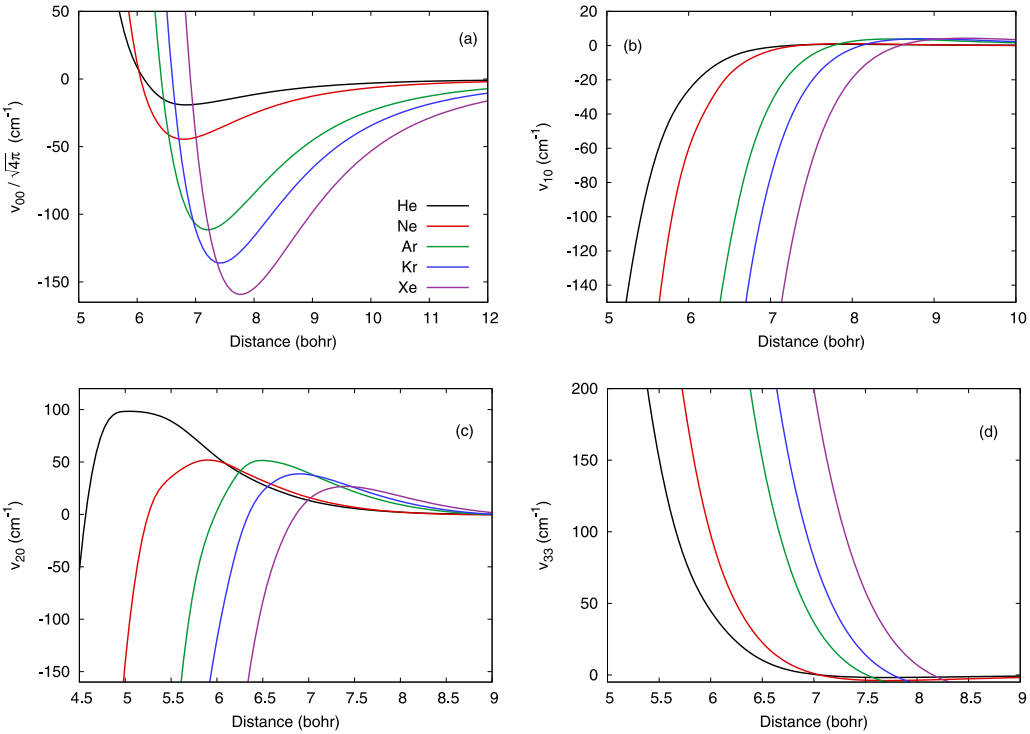

FIG. 1. Comparison of the dominant terms $v_{lm}(R, \rho_e)$ in the expansion of the NH_3–Rg PES for the five Rg atoms. (a) $v_{00}/\sqrt{4\pi}$, (b) v_{10}, (c) v_{20}, and (d) v_{33}.

corresponding to the inversion motion, given by

$$\hat{T}(\rho) = \frac{1}{2} g^{-\frac{1}{4}} \frac{\partial}{\partial_\rho} I_{\rho\rho}^{-1} g^{\frac{1}{2}} \partial_\rho g^{-\frac{1}{4}}, \quad (4)$$

where $g(\rho) = I_{xx} I_{yy} I_{zz} I_{\rho\rho}$ is expressed as a function of the principal inertia moments of ammonia and the moment of inertia $I_{\rho\rho}$ associated with the umbrella motion.[50] $V_{\text{umb}}(\rho)$ is the double-well potential for the umbrella motion, with a barrier at $\rho = \pi/2$. We used the same parametrization as in Ref. 25,

$$V_{\text{umb}}(\rho) = \frac{k_\rho}{2}\left(\rho - \frac{\pi}{2}\right)^2 + a_\rho \exp\left[-b_\rho\left(\rho - \frac{\pi}{2}\right)^2\right]. \quad (5)$$

Due to tunnelling through the barrier, the first two vibrational states are split into doublets. The three parameters are fitted in order to reproduce the experimental $v = 0 \rightarrow 1$ transition frequency (949.9 cm^{-1}) as well as the splittings in the $v = 0$ (0.79 cm^{-1}) and $v = 1$ (35.2 cm^{-1}) states. The parameters for NH_3–He are given in Ref. 25. For the other rare gases, we re-fitted the parameters to reflect the fact that the length of the N–H bonds used to compute the PES was slightly different. We used $k_\rho = 92\,026$ cm^{-1} rad^{-2}, $a_\rho = 23\,383$ cm^{-1}, and $b_\rho = 3.205$ rad^{-2}. For ND_3, the splittings are smaller (0.053 cm^{-1} in the $v = 0$ level) and the parameters are $k_\rho = 93\,170$ cm^{-1} rad^{-2}, $a_\rho = 23\,349$ cm^{-1}, and $b_\rho = 3.236$ rad^{-2}.

In our calculations, we kept the four lowest states $\phi_v^{\pm}(\rho)$ of the umbrella motion (where ± denotes the parity of the function under the inversion), corresponding to $v = 0$ and $v = 1$. We will compare the results obtained using the Hamiltonian (3) with those obtained with a model[1,37] that approximates the ground tunneling states as symmetric or antisymmetric combinations of the equilibrium structures, $|\pm\rangle = [f(\rho - \rho_e) \pm f(\pi - \rho + \rho_e)]/\sqrt{2}$, where $f(x)$ is a Dirac delta function localized at $x = 0$. This model only requires the knowledge of the PES at the equilibrium angle $\rho = \rho_e$ and has been shown to give accurate results[11,25] by direct comparison with the "exact" method using Hamiltonian (3). However, at collision energies lower than the inversion splitting (0.79 cm^{-1}), this approximation is not expected to be valid.

The inelastic scattering cross sections were computed using the quantum-mechanical close-coupling method, in which the total wave function is expanded as a sum of products of radial and angular functions. Upon integration over the angular coordinates, the Schrödinger equation leads to a set of coupled second-order differential equations to be solved using appropriate boundary conditions.[25] The total angular momentum J and its projection M on the space-fixed z axis are conserved during the collision.

The molecular symmetry group[51] of inverting NH_3, and also of the NH_3–Rg complexes, is $D_{3h}(M)$. NH_3 has two nuclear spin configurations depending on the value of k, the projection of the angular momentum j on the symmetry axis of the molecule. Rotational levels with $k = 0, 3, 6, \ldots$ (*ortho*-NH_3) correspond to the A_2 representations, while levels for which k is not a multiple of 3 (*para*-NH_3) correspond to the E representations. The levels corresponding to the A_1 representations are forbidden by nuclear spin statistics. The different spin configurations cannot interconvert during collisions. In the case of ND_3, there are no restrictions due to nuclear spin statistics, and states with $k = 0, 3, 6, \ldots$ can correspond either to the A_1 or the A_2 representations, so that there are three nuclear spin modifications.

The rotational levels of NH_3 and ND_3 are labeled as $|jk\pm\rangle$, where ± refers to the symmetry under inversion. The lowest energy levels of NH_3 are shown in Fig. 2.

B. Computational details

The four lowest levels $\phi_v^{\pm}(\rho)$ of the umbrella motion were calculated with the sinc-function discrete variable representation method.[52] Tests were performed with six umbrella functions, which showed that our calculations are converged. The coupled equations were solved with the renormalized Numerov propagator for energies in the range 0.001–300 cm^{-1}. The size of the grid in R, its number of points, and the maximum value of the total angular momentum J depended on the collision energy as well as on the colliding partners. Numerous tests were performed to make sure that the cross sections were converged. At the lowest energies considered, a typical grid ranged from 4 a_0 to 100 a_0, with the number of points increasing from about 200 for He to 600 for Xe. At the highest energies, we chose grids ranging from 4 a_0 to 30 a_0 with about 150–200 points for the various rare gases.

The maximum value of J required to obtain converged cross sections increased with the reduced mass of the system. At the highest energy, 45 partial waves were required to converge the elastic cross sections for NH_3–He, while for NH_3–Xe that number increased to 175. The convergence was faster for the inelastic cross sections. The size of the angular basis set was truncated at $j_{\max} = 7$ for NH_3 and $j_{\max} = 9$ for ND_3.

C. Results

For the reasons mentioned above, we will from now on focus on the initial state 11−. Unless otherwise stated, the

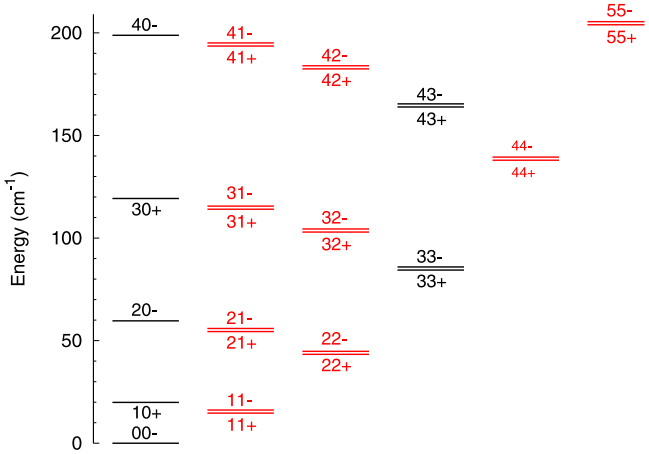

FIG. 2. Diagram of the lowest rotational energy levels of NH_3 labeled as $jk\pm$. The levels of *ortho*-NH_3 are shown in black while those of *para*-NH_3 are shown in red.

cross sections were calculated using the explicit treatment of the umbrella motion. The elastic ($11- \rightarrow 11-$) and inelastic ($11- \rightarrow jk\pm$) cross sections corresponding to scattering of NH_3 (top panel) or ND_3 (bottom panel) with neon atoms are shown in Fig. 3 for collision energies between 0 and 100 cm^{-1}. We note that the elastic cross section is much larger than the inelastic cross sections over the whole energy range. The 11+ state lies 0.79 cm^{-1} below the initial state 11− for NH_3 and 0.053 cm^{-1} for ND_3 and is therefore open at all collision energies.

We observe in Fig. 3 the opening of the various rotational channels, where the transition becomes energetically possible. At the threshold, the cross section increases sharply. For example, the 22+ channel opens up at a collision energy of 28.3 cm^{-1} for NH_3 and 14.7 cm^{-1} for ND_3, while the 22− channel is higher by the inversion splitting, 0.79 cm^{-1} for NH_3 and 0.053 cm^{-1} for ND_3. Other rotational levels become accessible at higher energies.

The relative magnitude of the cross sections can be understood by examining the expansion coefficients $v_{lm}(R, \rho)$ shown in Fig. 1, since they appear in the coupling matrix elements responsible for a given transition (apart from indirect processes).[1] For example, transitions which change the umbrella state of ammonia are caused by terms v_{lm} for which $l + m$ is odd, while the terms with even $l + m$ conserve the symmetry of the umbrella state. The elastic cross section depends on the v_{00} term, which is the dominant term for all rare gases, so that the elastic cross section is larger than the inelastic cross section. We observe from Fig. 3 that the inelastic cross section is dominated by the $11- \rightarrow 22-$ channel as soon as it becomes energetically possible. This transition is governed by the term v_{33}, which is large. On the other hand, the 22+ channel is not directly coupled to the 11− state by v_{33}, so its cross section is very small. The $11- \rightarrow 21-$ cross section is the second largest inelastic cross section at high energy and is controlled in first instance by the v_{20} coefficient. The $11- \rightarrow 11+$ transition is caused by the v_{10} term. While it is the only inelastic process at low collision energy, at high energy it is not the dominant cross section as the magnitude of other coefficients such as v_{33} and v_{20} is larger. In the case of ND_3, due to its smaller rotational constants, more channels are open in the energy range considered. We observe that the cross section $11- \rightarrow 44-$ becomes one of the leading inelastic cross sections as soon as this channel opens, which can be explained by the fact that this transition is also caused by the large v_{33} term.

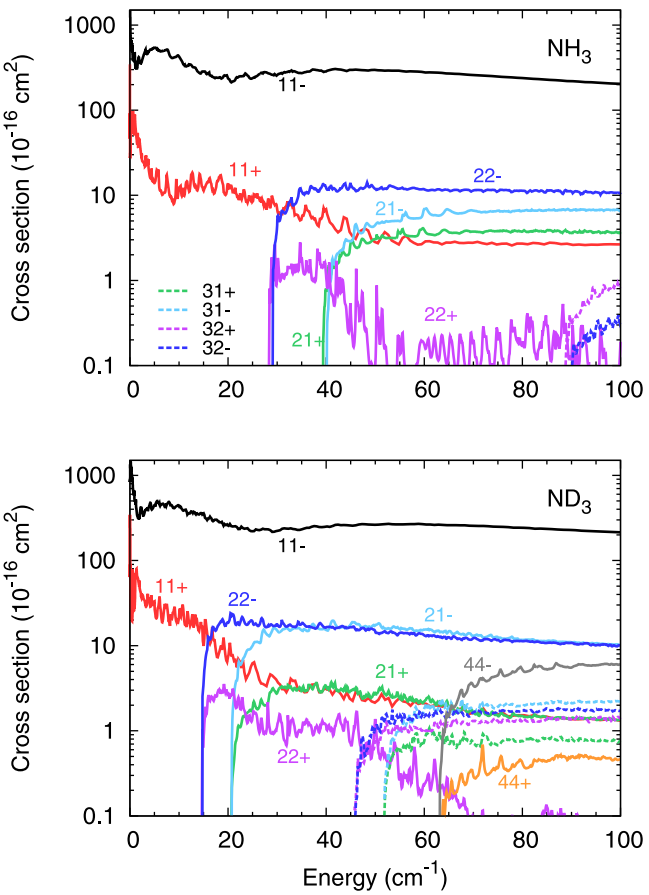

FIG. 3. Elastic and inelastic cross section for scattering of NH_3 (top) and ND_3 (bottom) in the initial state 11− by neon atoms.

The elastic and inelastic cross sections shown in Fig. 3 exhibit a large number of resonances which can be due either to quasi-bound states in the initial or final level (shape resonances) or due to other excited states (Feshbach resonances). In particular, it is well known that strong Feshbach resonances can occur at energies below the threshold corresponding to the opening of a new channel. Since ND_3 has more open channels at any given energy, the resonance structure is denser than in the case of NH_3. The effect of resonances (compared to the background cross section) is larger for the $11- \rightarrow 11+$ transition than for the $11- \rightarrow 22-$ transition, and it is possible that such resonances will soon be observed experimentally.[25] The $11- \rightarrow 22+$ cross section shows an even more pronounced resonance structure, but the fact that it is much smaller will make the measurements more difficult. The resonances are gradually suppressed as the energy increases.

The general features illustrated above for NH_3–Ne collisions are also valid for the other rare gases, but several trends along the Rg series are worth noting. First, the relative magnitude of the various inelastic cross sections is not always the same. For collisions of ammonia with helium, it was found[25] that the largest inelastic cross section corresponds to the excitation $11- \rightarrow 21-$, while for the other rare gases it is $11- \rightarrow 22-$ instead. The contribution to inelastic scattering of the cross section for the $11- \rightarrow 21-$ transition actually becomes smaller for heavier rare gases, which is related to the distinctive shape of the v_{20} coefficient that is responsible for this transition. This follows from the fact that although the expansion coefficients v_{lm} have the same shape for all the rare gases (see Fig. 1), their relative magnitude changes. Second, we have seen that the depth of the PES increases with the size of the rare gas, which implies the existence of quasi-bound states with higher energy. This in turn leads to the presence of shape resonances at higher collision energy for heavier rare gases, as will be further discussed below.

In Fig. 4, we compare the cross sections corresponding to the $11- \rightarrow 11-$ and $11- \rightarrow 11+$ transitions for NH_3 or ND_3

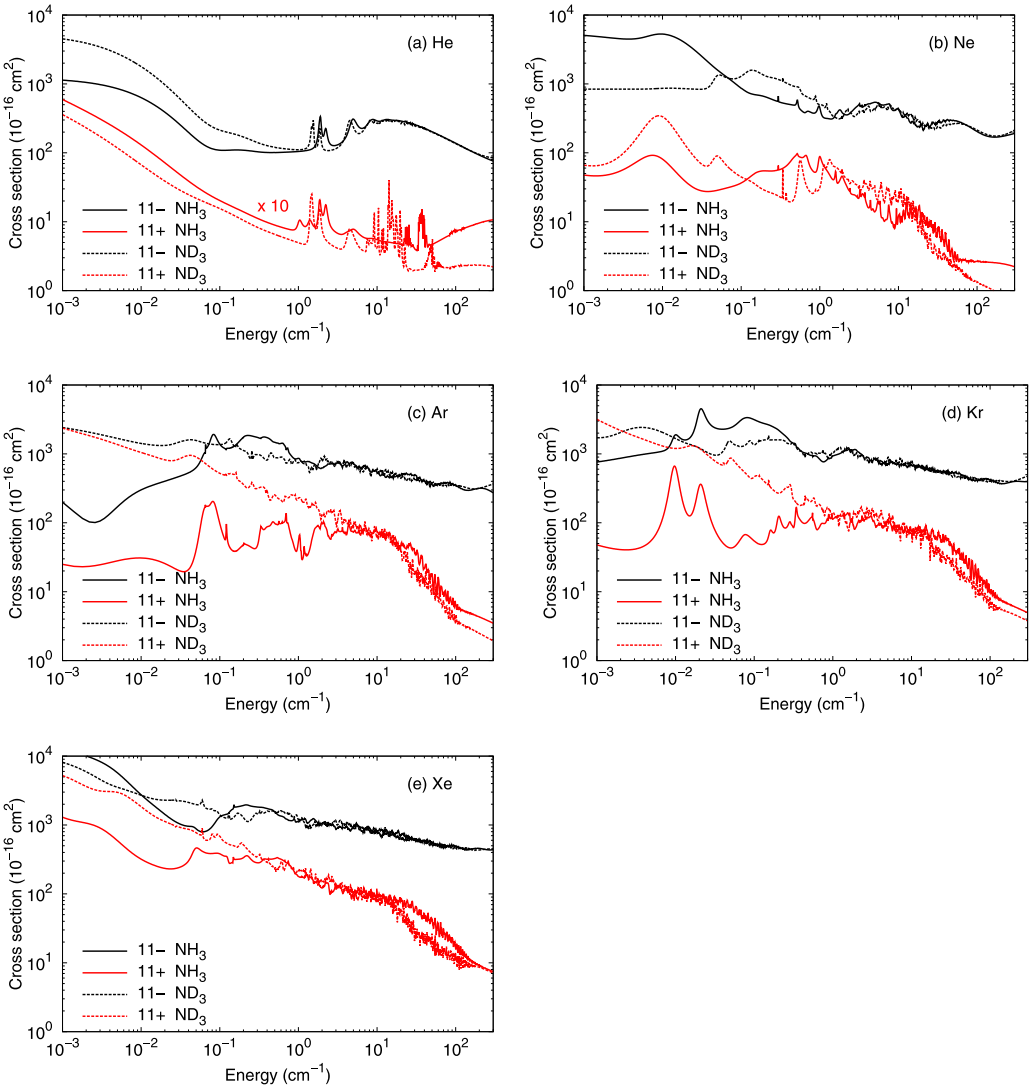

FIG. 4. Cross sections for elastic ($11- \rightarrow 11-$) and inelastic ($11- \rightarrow 11+$) scattering of NH_3 or ND_3 with rare gas atoms, with ammonia initially in the $11-$ state. (a) He, (b) Ne, (c) Ar, (d) Kr, and (e) Xe.

in collision with the five rare gases. In order to keep the same scale for all figures, the inelastic cross sections for helium were multiplied by a factor of 10.

To facilitate the analysis, we will distinguish two separate energy regimes. For energies $E > 10$ cm^{-1}, several trends can be distinguished in the cross sections: (i) The elastic cross section increases with the size of the rare gas. This is expected given that the magnitude of the corresponding expansion coefficient, v_{00}, also increases with size of the rare gas (see Fig. 1). The same conclusion applies to the inelastic cross section $11- \rightarrow 11+$, which depends mainly on the v_{10} coefficient. (ii) The elastic cross sections of NH_3 or ND_3 colliding with a given rare gas have similar magnitude, although the resonance structure differs. This is not the case for the inelastic $11- \rightarrow 11+$ cross section, which is in general larger for NH_3 as a colliding partner rather than ND_3. This can be explained by the fact that while the v_{00} coefficients are almost identical for NH_3 and ND_3, the v_{10} coefficients are larger for NH_3 compared to ND_3 (not shown). (iii) Because the depth of the PES increases with the size of the Rg, resonances occur at higher collision energies for the heavier Rg. (iv) The resonance structure is denser for ND_3 than for NH_3, both in the elastic and inelastic cross sections. As the mass of ND_3 is larger (and its rotational constants smaller) than NH_3, the number of quasi-bound states giving rise to resonances is larger.

Below $E = 10$ cm^{-1}, no clear trend appears. The energy at which the cross sections start to behave according to the Wigner threshold law, which implies that the elastic cross section becomes constant while the inelastic cross section is proportional to $1/\sqrt{E}$, depends on the colliding partners. For instance, at the lowest energy the elastic cross section for NH_3–He collisions is smaller than for ND_3–He, while the inelastic cross section is larger. On the other hand, for scattering of NH_3 or ND_3 with Ne or Xe, we reach the opposite conclusion. For Ar and Kr, both the elastic and the inelastic cross sections are larger for ND_3 than for NH_3 at the lowest energy considered here.

D. Effect of the umbrella motion

As discussed in Sec. III A, most scattering calculations involving ammonia are realized using a simple model[1,37]

that approximates the ground tunneling states as symmetric or antisymmetric combinations of the equilibrium structures. This approximation is expected to be accurate[11,25] and it is commonly applied either by choice (it simplifies the calculations and the umbrella motion is not expected to alter the dynamics at the collision energies considered) or by necessity, i.e., because the dependence of the PES on the umbrella coordinate was not considered. However, when the time scale of the collision becomes comparable to that of the inversion, the umbrella motion might affect the dynamics.

It was shown in Ref. 25 that for NH_3–He scattering the explicit description of the inversion motion and the model treatment gave very similar results even at energies as low as 10^{-4} cm^{-1}, although some subtle differences appeared in the shape of some resonances at higher energy. However, the same behaviour is not observed for other rare gases. The cross sections for the elastic and $11- \rightarrow 11+$ processes calculated using both approaches to inversion motion are compared for scattering of NH_3 with neon and argon atoms in Fig. 5. For both rare gases, we observe that the elastic and the inelastic cross sections are well represented by the model treatment for energies down to about 2 cm^{-1}. However, some discrepancies appear at lower energies. For NH_3–Ne collisions, these differences are at most 40% for elastic scattering and 80% for inelastic scattering down to 10^{-3} cm^{-1}. The effect is much more striking in the case of NH_3–Ar. At the lowest energy of 10^{-3} cm^{-1} considered here, the elastic cross section obtained by the model treatment is incorrect by a factor of 5, while there is a factor of almost 50 between the inelastic cross sections obtained by the two approaches. In the case of NH_3–Kr collisions, we also found significant differences (up to a factor of 10) in the cross sections below 1 cm^{-1} obtained with the two descriptions of the umbrella motion (not shown). However, for NH_3–Xe the difference is much smaller (a factor of 2 at most). The effect of the umbrella motion on the scattering cross sections thus cannot be simply reduced to a mass effect.

We also observed that the cross sections obtained with the elaborate treatment of the umbrella motion and only two umbrella functions were almost identical to those obtained with four functions. This implies that the difference between the model approach and the explicit treatment of the umbrella motion is due to the approximation of the matrix elements as $v_{lm}(R, \rho_e)$ in the model treatment rather than to the inclusion of higher-lying states $\phi_v^{\pm}(\rho)$.

Based on these findings, we recommend that the full treatment of the umbrella motion be applied in order to obtain accurate cross sections for scattering in the cold ($E < 1$ cm^{-1}) or ultracold ($E < 10^{-3}$ cm^{-1}) regimes.

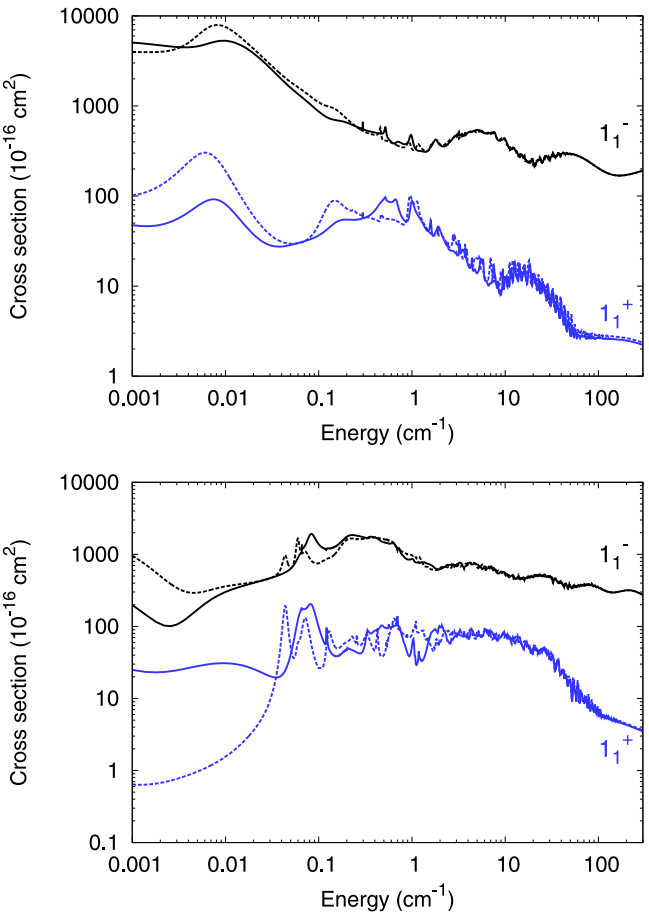

FIG. 5. Cross sections for $11- \rightarrow 11-$ (black) and $11- \rightarrow 11+$ (blue) transitions in collisions of NH_3 with neon (top) or argon (bottom). The full lines are results obtained with a full treatment of the umbrella motion, while the dashed lines are results obtained with the two state model (see text).

E. Sympathetic cooling of ammonia

The experimental preparation of cold (below 1 K) and ultracold (below 1 mK) molecules, when possible, promises many interesting applications that range from quantum information and precision measurements to the realization of many-body Hamiltonians.[53] Among the numerous schemes that have been devised to cool molecules, sympathetic cooling of Stark-decelerated molecules with laser-cooled atoms is very promising. In this method, the molecules are trapped either electrostatically or magnetically and thermalize by elastic collisions with the ultracold atoms. If the molecular species is not trapped in its absolute ground state, as is usually the case, inelastic collisions that remove molecules from the trap can also occur. In order for the cooling process to be efficient, elastic collisions should be much more frequent than inelastic collisions. It is usually assumed that the sympathetic cooling of a molecule by ultracold atoms is feasible if the ratio of elastic to inelastic cross sections is on the order 10–100 over the relevant range of temperature. The obvious choice of ultracold atoms are alkali atoms, since these can be routinely produced in the laboratory. Unfortunately, in most cases, inelastic collisions driven by anisotropic terms in the PES are too frequent and prevent an efficient cooling process.

In the case of NH_3, the state that can be trapped (the low-field seeking state) is the $11-$ state. Since the $11+$ channel is open at all collision energies, inelastic collisions $11- \rightarrow 11+$ can occur, which could prevent the cooling process. Zuchowski and Hutson previously examined the prospects for the cooling of NH_3 by thermalizing collisions with ultracold alkali-metal or alkaline earth metal atoms[32,54] and concluded that the interaction potentials in these systems were too anisotropic. They also discussed the case of NH_3–Xe

collisions, which they deemed more viable based on the low anisotropy of the PES.

Recently, Edmunds and Barker[31] demonstrated the realization of the trapping of argon atoms in the ground state by optically quenching them from a laser-cooled metastable state. The method can be applied to other rare gases[55] and opens the way for studying cold or ultracold NH_3–Rg collisions, as well as for sympathetic cooling of molecules such as ammonia. Indeed, the cooling process can be expected to be more favorable with rare gases as the PES is in general more isotropic than with alkali atoms.

From the discussion in Sec. III C, it can be anticipated that the lightest rare gases will provide the best prospects for sympathetic cooling. We have indeed seen that the magnitude of the anisotropic terms in the expansion of the PES, and in particular the v_{10} term responsible for $11- \rightarrow 11+$ transitions, increase with the size of the rare gas, leading to larger inelastic cross sections. However, the elastic cross section also increases so that the trend in the ratio $\sigma_{el}/\sigma_{inel}$ is uncertain.

We present in Fig. 6 the ratio $\sigma_{el}/\sigma_{inel}$ for the low energy scattering of NH_3 and ND_3 with the five rare gases. For energies in the range 10–100 cm^{-1}, we observe that the lighter rare gases provide larger ratios. However, this trend disappears in the cold regime where it depends on details of the PESs. In the case of NH_3, collisions with helium and neon provide the best prospects. For NH_3–He scattering, the ratio decreases from a value of about 500 at $E = 10$ cm^{-1} down to 20 at $E = 10^{-3}$ cm^{-1}. For NH_3–Ne collisions, the ratio is less than 10 at $E = 1$ cm^{-1}, but increases at lower energies and reaches 100 at $E = 10^{-3}$ cm^{-1}. The ratio $\sigma_{el}/\sigma_{inel}$ then decreases with decreasing collision energy due to the different threshold behavior of the elastic and inelastic cross sections.

In the case of ND_3, the ratio for collisions with helium is larger than 100 at most energies down to 10^{-3} cm^{-1} and provides the best option. The ratio for neon is about one order of magnitude smaller, while for the three heaviest Rg's it is even much smaller.

An important issue that arises when exploring the dynamics at low energy is that scattering cross sections strongly depend on details of the PES. In the (ultra)cold regime, the collision energy becomes smaller than the uncertainty in the PES that is due to the various approximations made in the electronic structure calculations. For this reason, it is useful to examine the sensitivity of the scattering cross sections to small variations in the PES. The simplest way to assess this sensitivity is to scale the PES by a factor λ and to compute the cross sections for various values of this parameter.[54]

We illustrate this sensitivity in Figs. 7 and 8, which show the dependence of the ratio $\sigma_{el}/\sigma_{inel}$ on λ for collisions of NH_3 with Ne and Ar. We have assumed a precision of 1% on the PES, so that λ is comprised between 0.99 and 1.01. Although the CCSD(T) method with the large basis set used in the *ab initio* calculations presented in Sec. II is accurate (as was demonstrated, for example, by comparing the computed spectrum of NH_3–Ar to measured data[33]), it is difficult to assess the precision of the PES with certainty. We use here the value of 1% for illustrative purposes.

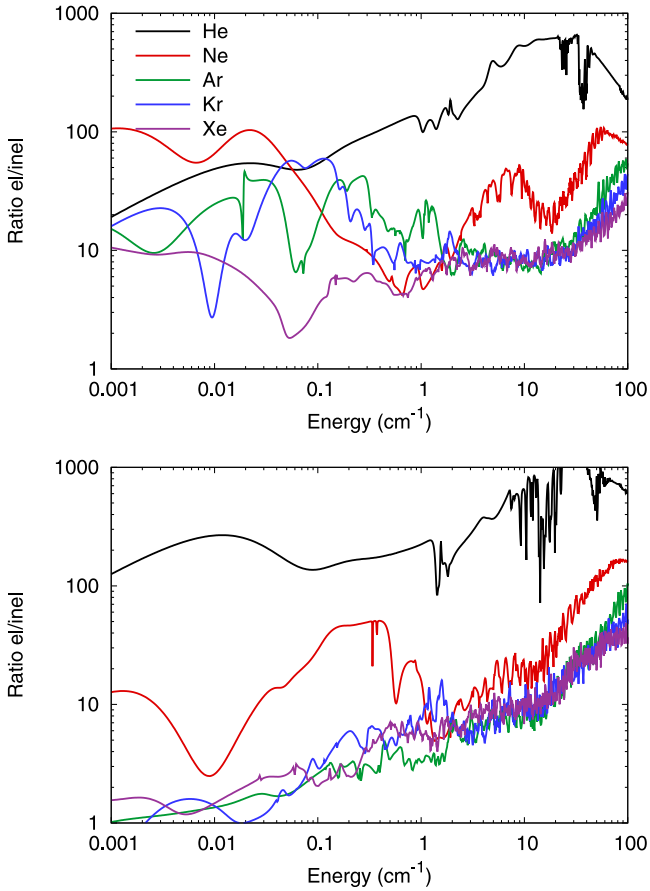

FIG. 6. Ratio $\sigma_{el}/\sigma_{inel}$ between elastic and inelastic cross sections for scattering of NH_3 (top) and ND_3 (bottom) in the 11− state with rare gas atoms.

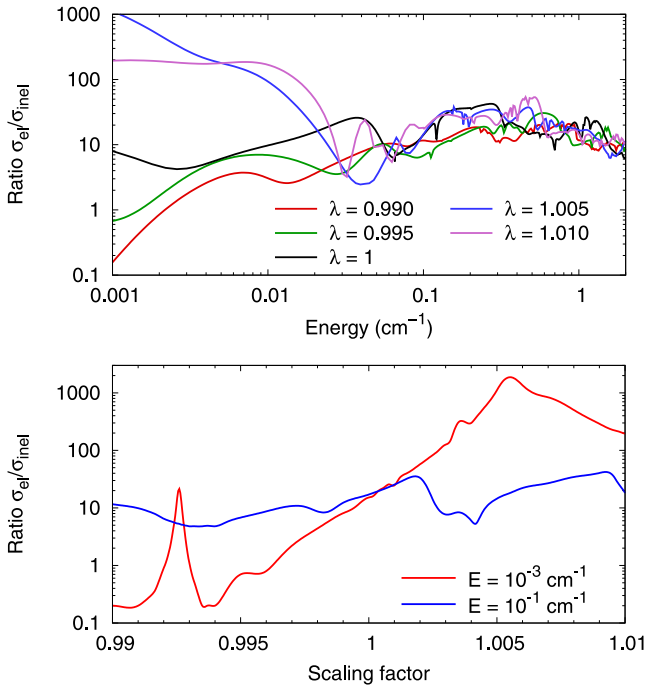

FIG. 7. Sensitivity of the ratio $\sigma_{el}/\sigma_{inel}$ to a scaling of the whole PES by a factor λ for NH_3–Ar collisions. Top panel: Ratio as a function of collision energy for several values of λ. Bottom panel: Ratio as a function of λ for two collision energies.

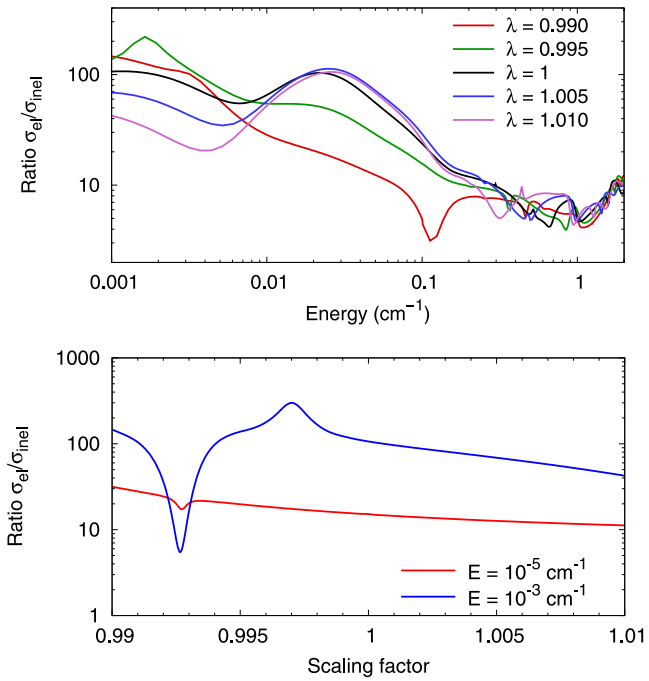

FIG. 8. Same as Fig. 7 but for NH_3–Ne.

Figure 7 shows a typical example of the sensitivity for NH_3–Ar collisions. We observe that the ratio $\sigma_{el}/\sigma_{inel}$ is relatively stable with respect to a change in λ down to an energy of 0.1 cm^{-1}. However, below 0.1 cm^{-1}, dramatic variations of the ratio can be seen, which are due to the occurrence of scattering resonances that depend very sensitively on the potential. At an energy of 10^{-3} cm^{-1}, the ratio varies by four orders of magnitude over the range of λ considered here (see Fig. 7, bottom panel). If the potential is scaled by 0.5%, the ratio reaches a value of 1000 (to be compared to the reference value of 10 for $\lambda = 1$), which would make collisions with argon an excellent prospect to cool NH_3. However, due to the extreme sensitivity as a function of λ, it is difficult to assess this possibility with confidence. Moreover, for energies in the range 0.1–10 cm^{-1}, the ratio $\sigma_{el}/\sigma_{inel}$ is of order 10, which is probably too small.

Figure 8 shows the ratio $\sigma_{el}/\sigma_{inel}$ for NH_3–Ne collisions, which represents the most promising prospect for sympathetic cooling of ammonia based on the results shown in Fig. 6. Similar to the case of NH_3–Ar collisions, the ratio is almost independent of λ down to collision energies of about 0.1 cm^{-1}. However, at lower energies the dependence of $\sigma_{el}/\sigma_{inel}$ on λ is much weaker than for NH_3–Ar. For example, at a collision energy of 10^{-3} cm^{-1}, the ratio is larger than 50 in most of the range of values of λ explored, although it decreases strongly around λ = 0.993 to less than 10. We repeated the calculations at an energy of 10^{-5} cm^{-1}, where the ratio $\sigma_{el}/\sigma_{inel}$ is larger than 10 for all values of λ, with a surprisingly weak dependence in the scaling parameter. These results show that the NH_3–Ne system is a good candidate for ammonia cooling even if the true PES would be slightly different from the one calculated in this study.

Finally, it should be noted that the dependence of the PES on a single scaling parameter λ is not sufficient to perform a full sensitivity analysis of the scattering cross sections since the anisotropy of the PES does not change. A more complete analysis would be desirable and could be performed, for example, using the method recently presented by Cui and Krems[56] in order to assess more thoroughly the possibility of sympathetic cooling of NH_3 and ND_3. However, we note that since the value of the ratio $\sigma_{el}/\sigma_{inel}$ is only weakly dependent on λ for collision energies above 0.1 cm^{-1}, He and Ne would still provide the best prospects, as illustrated in Fig. 6.

In the context of possible future experiments, the effect of the trapping field should also be considered. In the cold regime, it is expected that the presence of a field will result in smaller elastic cross sections and larger inelastic cross sections compared to the field-free case.[57] This would lead to a decrease of the ratio $\sigma_{el}/\sigma_{inel}$ and could cause the cooling process to be less efficient even for the favorable cases discussed above. On the other hand, at higher energies the effect of the field on the cross sections, and particularly on the resonance structure discussed in Sec. III C, is anticipated to be small.

IV. CONCLUSIONS

We have presented calculations on the elastic and rotationally inelastic scattering of NH_3 and ND_3 with rare gas atoms. We obtained scattering cross sections by means of the quantum close-coupling method for collision energies between 0.001 and 300 cm^{-1} while taking the inversion motion of NH_3 explicitly into account.

The scattering calculations were performed using accurate four-dimensional *ab initio* potential energy surfaces that depend explicitly on the umbrella angle of NH_3. For the NH_3–He and NH_3–Ar systems, we used previously reported PESs, while the PESs of the NH_3–Ne, NH_3–Kr, and NH_3–Xe complexes were computed in this work using the CCSD(T) method with large basis sets. We constructed fits of the PESs that include an accurate description of the long-range behaviour. We identified the main features of the PESs as well as the trends along the rare gas series, and compared them to previous studies.

The cross sections for scattering of NH_3 and ND_3 with rare gas atoms were obtained for the initial state $jk\pm = 11-$ of ammonia, which is amenable to Stark deceleration and electrostatic trapping. We showed that a rich resonance structure, composed of shape and Feshbach resonances, is present in the inelastic cross sections. Such resonances can probably be observed in future experiments using Stark decelerated molecular beams of ammonia. The relative magnitude of the cross sections for the various inelastic channels can be explained in terms of the coefficients $v_{lm}(R,\rho)$ that appear in the expansion of the anisotropic PES in spherical harmonics. In particular, we showed that the magnitude of the $11- \rightarrow 11+$ inelastic cross sections increases with the size of the rare gas atom, and that the cross section is larger when the colliding partner is NH_3 rather than ND_3. We also examined the validity of a commonly used model treatment of the ammonia umbrella motion at low collision energy. We found that while the model performs very well for NH_3–He, as was previously reported,[25] large discrepancies with the explicit

treatment of the umbrella motion can occur for scattering of NH_3 with the other Rg atoms at collision energies below 1 cm^{-1}.

Finally, we investigated the possibility of using cold or ultracold rare gas atoms in order to sympathetically cool NH_3 or ND_3 molecules. We found that the largest values for the ratio of elastic to inelastic cross sections are obtained for the NH_3–Ne and ND_3–He systems, which thus seem to offer the best prospects for the experimental realization of sympathetic cooling of ammonia.

ACKNOWLEDGMENTS

The work of J.L. is supported by the Belgian Fund for Scientific Research–FNRS. J.L. thanks J. Liévin and N. Vaeck for useful discussions, as well as the Wiener-Anspach Foundation (ACME project). The calculations presented in this work have been performed using the Hydra and Vega computing clusters at the ULB/VUB.

[1]S. Green, J. Chem. Phys. **64**, 3463 (1976).
[2]L. Machin and E. Roueff, J. Phys. B: At., Mol. Opt. Phys. **38**, 1519 (2005).
[3]B. Yang and P. C. Stancil, Eur. Phys. J. D **47**, 351 (2008).
[4]H. Meyer, U. Buck, R. Schinke, and G. H. F. Diercksen, J. Chem. Phys. **84**, 4976 (1986).
[5]J. Schleipen and J. ter Meulen, Chem. Phys. **156**, 479 (1991).
[6]G. Fraser, D. Nelson, Jr., A. Charo, and W. Klemperer, J. Chem. Phys. **82**, 2535 (1985).
[7]E. Zwart, H. Linnartz, W. Meerts, G. Fraser, D. Nelson, Jr., and W. Klemperer, J. Chem. Phys. **95**, 793 (1991).
[8]C. Schmuttenmaer, J. Loeser, and R. Saykally, J. Chem. Phys. **101**, 139 (1994).
[9]K. Didriche, T. Földes, T. Vanfleteren, and M. Herman, J. Chem. Phys. **138**, 181101 (2013).
[10]J. Schleipen, J. ter Meulen, G. van der Sanden, P. Wormer, and A. van der Avoird, Chem. Phys. **163**, 161 (1992).
[11]G. van der Sanden, P. Wormer, A. van der Avoird, J. Schleipen, and J. ter Meulen, J. Chem. Phys. **97**, 6460 (1992).
[12]G. van der Sanden, P. Wormer, A. van der Avoird, C. Schmuttenmaer, and R. Saykally, Chem. Phys. Lett. **226**, 22 (1994).
[13]G. van der Sanden, P. Wormer, and A. van der Avoird, J. Chem. Phys. **105**, 3079 (1996).
[14]H. Meyer, J. Chem. Phys. **101**, 6697 (1994).
[15]C. Ayari, J. Loreau, M. Dhib, C. Daussy, and H. Arouia, J. Mol. Spectrosc. (published online).
[16]J. van Wijngaarden and W. Jäger, J. Chem. Phys. **115**, 6504 (2001).
[17]J. van Wijngaarden and W. Jäger, Mol. Phys. **99**, 1215 (2001).
[18]Q. Wen and W. Jäger, J. Chem. Phys. **128**, 204309 (2008).
[19]T. Vanfleteren, T. Földes, J. Liévin, and M. Herman, Mol. Phys. (published online).
[20]J. Kay, S. Y. T. van de Meerakker, E. Wade, K. Strecker, and D. Chandler, J. Phys. Chem. A **113**, 14800 (2009).
[21]F. Pirani, L. Roncaratti, L. Belpassi, F. Tarantelli, and D. Cappelletti, J. Chem. Phys. **135**, 194301 (2011).
[22]O. Tkac, A. K. Saha, J. Onvlee, C.-H. Yang, G. Sarma, C. K. Bishwakarma, S. Y. T. van de Meerakker, A. van der Avoird, D. H. Parker, and A. J. Orr-Ewing, Phys. Chem. Chem. Phys. **16**, 477 (2014).
[23]O. Tkac, A. K. Saha, J. Loreau, D. H. Parker, A. van der Avoird, and A. J. Orr-Ewing, J. Phys. Chem. A **119**, 5979 (2015).
[24]O. Tkac, A. K. Saha, J. Loreau, Q. Ma, P. J. Dagdigian, D. H. Parker, A. van der Avoird, and A. J. Orr-Ewing, Mol. Phys. (published online).
[25]K. B. Gubbels, S. Y. T. van de Meerakker, G. C. Groenenboom, G. Meijer, and A. van der Avoird, J. Chem. Phys. **136**, 074301 (2012).
[26]Q. Ma, A. van der Avoird, J. Loreau, M. Alexander, S. Y. T. van de Meerakker, and P. J. Dagdigian, J. Chem. Phys. **143**, 044312 (2015).
[27]A. von Zastrow, J. Onvlee, S. N. Vogels, G. C. Groenenboom, A. van der Avoird, and S. Y. T. van de Meerakker, Nat. Chem. **6**, 216 (2014).
[28]S. Y. T. van de Meerakker, H. L. Bethlem, N. Vanhaecke, and G. Meijer, Chem. Rev. **112**, 4828 (2012).
[29]K. S. Twyman, M. T. Bell, B. R. Heazlewood, and T. P. Softley, J. Chem. Phys. **141**, 024308 (2014).
[30]O. Schullian, J. Loreau, N. Vaeck, A. van der Avoird, B. R. Heazlewood, C. J. Rennick, and T. P. Softley, Mol. Phys. (published online).
[31]P. Edmunds and P. F. Barker, Phys. Rev. Lett. **113**, 183001 (2014).
[32]P. Żuchowski and J. M. Hutson, Phys. Rev. A **78**, 022701 (2008).
[33]J. Loreau, J. Liévin, Y. Scribano, and A. van der Avoird, J. Chem. Phys. **141**, 224303 (2014).
[34]J. Loreau, AIP Conf. Proc. **1618**, 585 (2014).
[35]G. Chalasinski, M. Szczesniak, and S. Scheiner, J. Chem. Phys. **97**, 8181 (1992).
[36]G. Bistoni, L. Belpassi, F. Tarantelli, F. Pirani, and D. Cappelletti, J. Phys. Chem. A **115**, 14657 (2011).
[37]S. L. Davis and J. E. Boggs, J. Chem. Phys. **69**, 2355 (1978).
[38]C. Hampel, K. Peterson, and H. J. Werner, Chem. Phys. Lett. **190**, 1 (1992).
[39]H.-J. Werner, P. J. Knowles, G. Knizia, F. R. Manby, M. Schütz *et al.*, MOLPRO, version 2012.1, a package of *ab initio* programs, 2012, see http://www.molpro.net.
[40]T. H. Dunning, Jr., J. Chem. Phys. **90**, 1007 (1989).
[41]S. M. Cybulski and R. R. Toczylowski, J. Chem. Phys. **111**, 10520 (1999).
[42]K. A. Peterson, D. Figgen, E. Goll, H. Stoll, and M. Dolg, J. Chem. Phys. **119**, 11113 (2003).
[43]S. F. Boys and F. Bernardi, Mol. Phys. **19**, 553 (1970).
[44]J. Loreau, H. R. Sadeghpour, and A. Dalgarno, J. Chem. Phys. **138**, 084301 (2013).
[45]T. J. Lee and P. R. Taylor, Int. J. Quantum Chem. **36**(S23), 199 (1989).
[46]D. Jayatilaka and T. J. Lee, J. Chem. Phys. **98**, 9734 (1993).
[47]T. J. Lee, Chem. Phys. Lett. **372**, 362 (2003).
[48]See supplementary material at http://dx.doi.org/10.1063/1.4935259 for the *ab initio* data points of the NH_3-Ne, NH_3-Kr, and NH_3-Xe PESs.
[49]C. Schmuttenmaer, R. Cohen, and R. Saykally, J. Chem. Phys. **101**, 146 (1994).
[50]J. van Bladel, A. van der Avoird, and P. Wormer, Chem. Phys. **165**, 47 (1992).
[51]P. R. Bunker and P. Jensen, *Molecular Symmetry and Spectroscopy*, 2nd ed. (NRC Research Press, Ottawa, 1998).
[52]D. T. Colbert and W. H. Miller, J. Chem. Phys. **96**, 1982 (1992).
[53]*Cold Molecules*, edited by R. V. Krems, B. Friedrich, and W. C. Stwalley (CRC Press, 2009).
[54]P. Żuchowski and J. M. Hutson, Phys. Rev. A **79**, 062708 (2009).
[55]P. F. Barker, S. M. Purcell, P. Douglas, P. Barletta, N. Coppendale, C. Maher-McWilliams, and J. Tennyson, Faraday Discuss. **142**, 175 (2009).
[56]J. Cui and R. V. Krems, Phys. Rev. Lett. **115**, 073202 (2015).
[57]L. P. Parazzoli, N. J. Fitch, P. S. Żuchowski, J. M. Hutson, and H. J. Lewandowski, Phys. Rev. Lett. **106**, 193201 (2011).